REPORT DOCUMENTATION PAGE

Form Approved
OMB No. 0704-0188

2. REPORT DATE	3. REPORT TYPE AND DATES COVERED
December 1991	professional paper

4. TITLE AND SUBTITLE

ADVANCED BEAMFORMING CONCEPTS: SOURCE LOCALIZATION USING THE BISPECTRUM, GABOR TRANSFORM, WIGNER-VILLE DISTRIBUTION, AND NONSTATIONARY SIGNAL REPRESENTATIONS

5. FUNDING NUMBERS

In-house

6. AUTHOR(S)

J. C. Allen

7. PERFORMING ORGANIZATION NAME(S) AND ADDRESS(ES)

Naval Ocean Systems Center
San Diego, CA 92152–5000

8. PERFORMING ORGANIZATION REPORT NUMBER

9. SPONSORING/MONITORING AGENCY NAME(S) AND ADDRESS(ES)

Naval Ocean Systems Center
San Diego, CA 92152–5000

10. SPONSORING/MONITORING AGENCY REPORT NUMBER

11. SUPPLEMENTARY NOTES

12a. DISTRIBUTION/AVAILABILITY STATEMENT

Approved for public release; distribution is unlimited.

12b. DISTRIBUTION CODE

13. ABSTRACT *(Maximum 200 words)*

Power spectral estimation provides one approach to direction-finding. This approach readily generalizes to produce a collection of newer direction-finding algorithms. Estimation of the bispectrum yields a bispectral direction finder. Estimates of time-frequency distributions produce Wigner-Ville and Gabor direction-finders. Some types of non-stationary time series admit spectral estimators which can be used to localize a source. Chaotic signals can also be localized using recently developed parameter estimators.

Published in the *Proceedings of the 25th Asilomar Conference on Signal, Systems, and Computers*, November, 1991.

14. SUBJECT TERMS

15. NUMBER OF PAGES

16. PRICE CODE

17. SECURITY CLASSIFICATION OF REPORT	18. SECURITY CLASSIFICATION OF THIS PAGE	19. SECURITY CLASSIFICATION OF ABSTRACT	20. LIMITATION OF ABSTRACT
UNCLASSIFIED	UNCLASSIFIED	UNCLASSIFIED	SAME AS REPORT

21a. NAME OF RESPONSIBLE INDIVIDUAL	21b. TELEPHONE (include Area Code)	21c. OFFICE SYMBOL
J. C. Allen	(619) 553-6566	Code 575

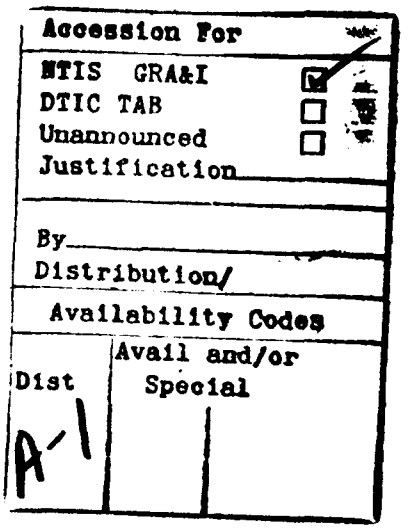

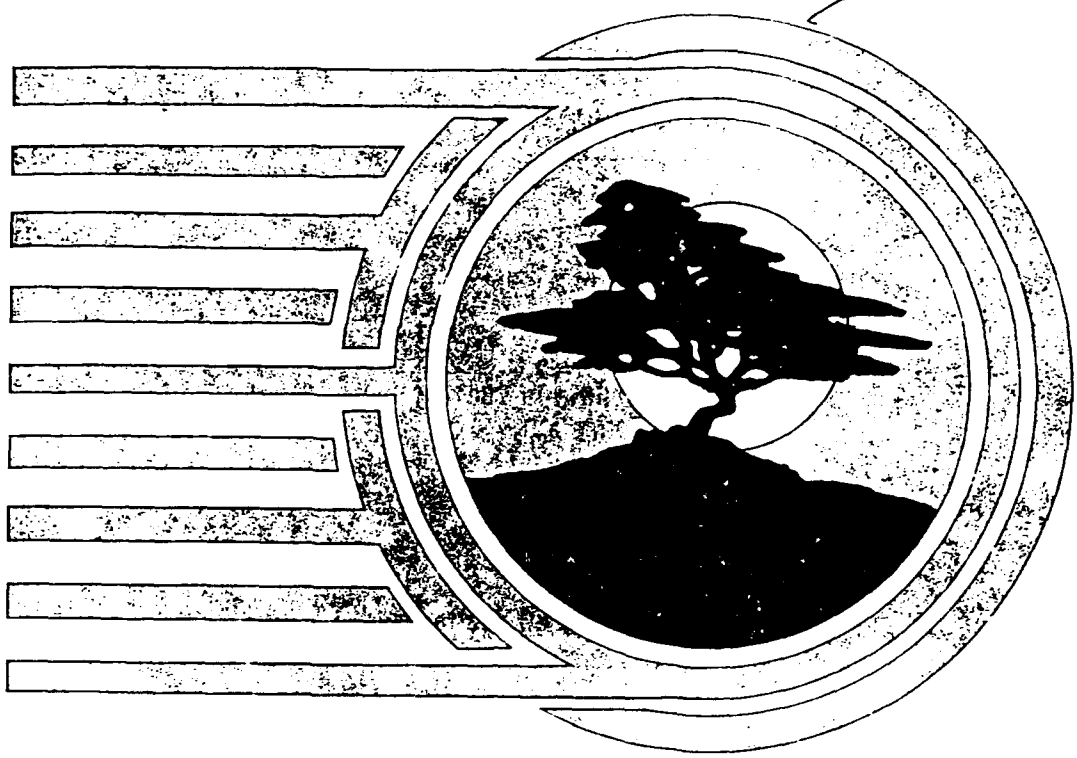

Twenty-Fifth
Asilomar Conference on
Signal, Systems & Computers

November 4 - 6, 1991

FINAL PROGRAM & ABSTRACTS

Asilomar Hotel
Conference Grounds

THE COMPUTER SOCIETY
OF THE IEEE

THE INSTITUTE OF ELECTRICAL AND
ELECTRONICS ENGINEERS INC

Advanced Beamforming Concepts: Source Localization Using the Bispectrum, Gabor Transform, Wigner-Ville Distribution, and Nonstationary Signal Representations

Jeffery C. Allen
Naval Ocean Systems Center
San Diego, CA 92152–5000
TP4-3

Abstract

Power spectral estimation provides one approach to direction-finding. This approach readily generalizes to produce a collection of newer direction-finding algorithms. Estimation of the bispectrum yields a bispectral direction finder. Estimates of time-frequency distributions produce Wigner-Ville and Gabor direction-finders. Some types of non-stationary time series admit spectral estimators which can be used to localize a source. Chaotic signals can also be localized using recently developed parameter estimators.

1 Introduction

In 1982, Don Johnson wrote a much-cited paper entitled *The Application of Spectral Estimation Methods to Bearing Estimation Problems* [10]. In the intervening years, considerable development has taken place in time-frequency distributions, higher-order statistics, and estimators for non-stationary random process. This paper extends the theme developed by Johnson to encompass some of these newer results. Following a review of conventional direction-finding (DF), section 3 shows how estimators of the bispectrum can yield DF algorithms. DF using the Gabor Transform and Wigner-Ville Distribution (WVD) are covered in sections 4 and 5. Spectral estimators for time series which are periodically correlated (cyclostationary) also yield a DF algorithm (section 6) as do the estimators for a fractral-like time series (section 7).

Vectors are denoted boldface $\mathbf{x}$. The conjugate transpose is denoted as $\mathbf{x}^H$. The normal or Gaussian distribution with mean μ and variance σ_2 is denoted $\mathcal{N}(\mu, \sigma^2)$. If $\{\mathbf{x}(t)\}$ is a zero-mean, vector-valued random process, the covariance function is

$$R_{\mathbf{x}}(t_1, t_2) = E[\mathbf{x}(t_1)\mathbf{x}(t_2)^H],$$

and the cross spectral density (CSD) matrix is:

$$P_{\mathbf{x}}(f_1, f_2) = \int_{-\infty}^{\infty}\int_{-\infty}^{\infty} e^{-i2\pi(f_1 t_1 - f_2 t_2)} R_{\mathbf{x}}(t_1, t_2)\, dt_1\, dt_2.$$

Table 1: Principal Notation

t	time
f	frequency
c	speed of sound
E	expectation operator
$\mathbf{u}$	unit (look) vector
$x_m(t)$	mth sensor output
$\mathbf{x}(t) = [x_m(t)]$	array "snapshots"
$\mathbf{r}_m$	vector to mth sensor
$\mathbf{a}(f, \mathbf{u}) = [\exp(i2\pi f \mathbf{r}_m^H \mathbf{u}/c)]$	steering vector

2 Conventional DF

A quick review of conventional DF is undertaken in this section to provide the nomenclature for the subsequent DF algorithms. Assume a single source is transmitting a signal $s(t)$ in a lossless, plane-wave environment in the direction $-\mathbf{u}_0$. The signal $s(t)$ is received by M omni-directional sensors fixed at positions $\mathbf{r}_m$. Each sensor receives a time-delayed copy of $s(t)$. The time delay function associated with the mth sensor is $\tau_m(\mathbf{u}_0) = \mathbf{r}_m^H \mathbf{u}_0/c$. If additive noise $(z_m(t))$ is present at the mth sensor, then the noise-corrupted signal at the m-th sensor is determined as [10]:

$$x_m(t) = s(t + \tau_m(\mathbf{u}_0)) + z_m(t). \qquad (1)$$

The classical DF output $x(t, \mathbf{u})$ using look vector $\mathbf{u}$ is determined by weights (w_m) and time delays $(\tau_m(\mathbf{u}))$ as

$$x(t, \mathbf{u}) = \sum_{m=1}^{M} w_m x_m(t - \tau_m(\mathbf{u})). \qquad (2)$$

The fundamental point of Johnson's paper [10] is that the estimates of the power spectrum of $\{x(t, \mathbf{u})\}$ yield bearing estimates. To see this, make the following standard assumptions regarding the stationarity of the signal and the noise process $z(t) = [z_m(t)]$.

Assumption 2.1 Single source, uncorrelated noise:

1. the plane-wave signal $s(t)$ is a zero-mean, wide-sense stationary (WSS) random process.

2. the noise $\mathbf{z}(t)$ is a zero-mean, wide-sense stationary random process.

3. the signal $s(t)$ and the sensor noise are uncorrelated.

If $s(t)$ WSS, it admits a mean-square Fourier representation

$$s(t) = \int_{-\infty}^{\infty} e^{i2\pi ft} dS(f),$$

where $dS(f)$ is an orthogonally scattered measure [12]. The power spectrum $P_s(f)$ of the signal is determined by $dP_s(f) = E[|dS(f)|^2]$. Likewise, the WSS noise vector $\mathbf{z}(t)$ admits Fourier representation with an orthogonally scattered vector measure $d\mathbf{Z}(f)$ and its CSD matrix is given by $dP_{\mathbf{Z}}(f) = E[d\mathbf{Z}(f)d\mathbf{Z}(f)^H]$. Under the assumptions 2.1, it may be shown that the array output $\{\mathbf{x}(t)\}$ admits an orthogonally scattered vector measure [10]:

$$d\mathbf{X}(f) = \mathbf{a}(f, \mathbf{u}_0)dS(f) + d\mathbf{Z}(f). \quad (3)$$

Likewise, it may also be shown that the CSD matrix of the array output is given as

$$\begin{aligned} dP_{\mathbf{X}}(f) &= E[d\mathbf{X}(f)d\mathbf{X}(f)^H] \\ &= \mathbf{a}(f, \mathbf{u}_0)\mathbf{a}(f, \mathbf{u}_0)^H dP_s(f) + dP_{\mathbf{Z}}(f) \end{aligned} \quad (4)$$

Then the power spectrum $P_x(f, \mathbf{u})$ of the classical delay-sum DF is given by [1]: $P_x(f, \mathbf{u}) = \mathbf{a}(f, \mathbf{u})^H W P_{\mathbf{X}}(f) W \mathbf{a}(f, \mathbf{u})$, where W is the diagonal matrix of the weights. As a special case, suppose the sensor noises are independent and identically distributed so that $P_z(f)$ is a scalar multiple of the identity matrix. In this case, $P_x(f, \mathbf{u}_0)$ is the maximum value and illustrates the idea behind DF: *that the source direction can be determined by examining the maximum $P_x(f, \mathbf{u})$ as a function of the "look vector" $\mathbf{u}$* .

As pointed out by Johnson [10], obtaining the CSD matrix $P_{\mathbf{X}}(f)$ is basic to this classical DF, as well as the MVDR and MUSIC DF. Therefore, *consistent estimation of the CSD matrix is a key point in these DF methods* and is usually justified on explicit WSS assumptions and implicit ergodic assumptions. Before we consider those cases where the array output $\{x(t)\}$ is non-stationary, the next section is devoted to showing how to generalize DF via the power spectrum to DF via the bispectrum.

3 Bispectral DF

Higher-order statistical analysis of time series has been undergoing a tremendous development in the last decade. Excellent review articles of this area are [13], [14], while [19] and [18] are foundational texts. In addition, Forster and Nikias [3] have produced a MVDR-like DF based on the bispectrum while Porat and Friedlander [16] DF using fourth-order cumulants. In this section, we show how to obtain a bispectral MUSIC DF and a mixed bispectral MUSIC DF.

Definition 3.1 [13] If $\{\mathbf{x}(t)\}$ is a zero-mean, third-order stationary random process, then one definition of the third-order cumulant is

$$C_{\mathbf{X}}(\tau_1, \tau_2) = E[\mathbf{x}(t + \tau_1) \otimes \mathbf{x}(t + \tau_2) \otimes \overline{\mathbf{x}(t)}],$$

where $\otimes$ is the Kronecker product. The cross bispectral density tensor (CBT) is:

$$B_{\mathbf{X}}(f_1, f_2) = \int_{-\infty}^{\infty}\int_{-\infty}^{\infty} e^{-i2\pi(f_1\tau_1 + f_2\tau_2)} C_{\mathbf{X}}(\tau_1, \tau_2) d\tau_1 d\tau_2.$$

The generalization of equation (3) for the CSD matrix of the array output $\{\mathbf{x}(t)\}$ to the CBT is straightforward [19]:

$$dB_{\mathbf{X}}(f_1, f_2) = E[d\mathbf{X}(f_1) \otimes d\mathbf{X}(f_2) \otimes \overline{d\mathbf{X}(f_1 + f_2)}]. \quad (5)$$

For DF using the bispectrum, the classical assumptions 2.1 need to be modified:

Assumption 3.1 Single source, independent Gaussian noise:

1. the plane-wave signal $s(t)$ is a zero-mean, third-order stationary random process.

2. the noise $\mathbf{z}(t)$ is a zero-mean, Gaussian, *WSS random process.*

3. the signal $s(t)$ and the sensor noise are independent.

The bispectrum of a Gaussian WSS is zero [19, page 36]. From equation (3), equation (5), and assumption 3.1, it can be shown that

$$dB_{\mathbf{X}}(f_1, f_2) = \mathbf{a}(f_1, \mathbf{u}_0) \otimes \mathbf{a}(f_2, \mathbf{u}_0) \otimes \overline{\mathbf{a}(f_1 + f_2, \mathbf{u}_0)} dB_{\mathbf{X}}(f_1, f_2).$$

In this form, the third-order signal subspace is obvious. For computational purposes, we can use the equivalent form for three tensors: $\mathbf{x} \otimes \mathbf{y} \otimes \overline{\mathbf{z}} \sim (\mathbf{x} \otimes \mathbf{y})\mathbf{z}^H$, which permits the application of the SVD to determine the projections for the third-order signal and noise subspaces. Moreover, this equivalence combined with equation (5) indicates that the CBT may be estimated by averaging Kronecker products of the DFT obtained by segmenting the data into time blocks [14].

Bispectral MUSIC performs DF by projecting a steering vector onto the third-order noise subspace and calculating the reciprocal of the norm of the projection. Mixed bispectral MUSIC performs DF by projecting a steering vector onto the second-order noise subspace (standard MUSIC) followed by the projection into the third-order noise subspace and then calculating the reciprocal of the norm.

The following simulation provides an assessment of these DF methods. A 10-sensor linear array is laid along the x-axis. Each sensor is spaced one-half wave length at 11 Hertz. The standard right-hand coordinate system is assumed so that broadside to the array measure $\theta = 90°$. A Gaussian and a bilinear signal were present. The Gaussian signal was generated

by AR filtering i.i.d. $\mathcal{N}(0,1)$ noise (AR coefficients: a_0=1, a_1=.9, a_2=.81). This signal was normalized by setting the sample variance to 1. It arrived on the array from 80° azimuth using an FFT to perform the lag. The bilinear signal was generated using the bilinear model of Gabr [5]: $s_t = 1.3 s_{t-3}\epsilon_{t-3} + \epsilon_t$, where $\{\epsilon_t\}$ is i.i.d. $\mathcal{N}(0,1)$ and then normalized by setting the sample variance to 1. It arrived on the array from 100° azimuth using an FFT to perform the lag. Finally, the sensor noise was modeled as i.i.d. $\mathcal{N}(0,1)$. The sample rate was 34.38 Hertz and a total of 16,384 array snapshots were collected.

The classical, MUSIC, bispectral MUSIC and mixed bispectral MUSIC DF were applied to this data. All CSD and CBT estimates were made with 32-sample block averaging assuming f_1=f_2=11.5 Hertz. All MUSIC-type DF assumed two signals present. The results are plotted in figure 1. The classical, MUSIC, and mixed bispectral MUSIC indicate both sources with the primary lobe at the Gaussian source while the bispectral MUSIC appears to discriminate between the Gaussian and the bilinear source.

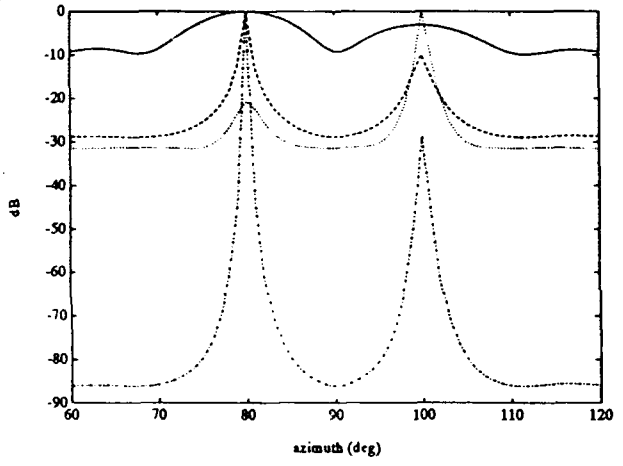

Figure 1: **Bispectral DF on Two Sources** — Gaussian source at 80° azimuth; bilinear source at 100° azimuth; Gaussian sensor noise. The solid line is the classical DF, the dashed line is MUSIC, the dotted line is bispectral MUSIC, and the dash-dot line is mixed bispectral MUSIC.

4 DF via the Gabor Transform

This section shows how the Gabor transform can be used as a pre-filter for removing transient signals corrupting the sensor data. Since a transient can be isolated from the sensor data, it follows that the same processing can apply to transient DF [22, Chapter 4] and admit more advanced transient DF based on minimum-variance or subspace methods. For brevity, we focus on using the Gabor transform as a pre-filter.

The application of the Gabor transform as a means of transient detection was beautifully developed by Friedlander and Porat [4] and we borrow heavily from that paper. Let $y(t)$ be a given continuous-time, real-valued signal. Let $g(t)$ be a fixed, non-negative function of unit area, called the window function. Then the Gabor representation of $y(t)$ using the window function $g(t)$ is

$$y(t) = \sum_{m=-\infty}^{\infty} \sum_{n=-\infty}^{\infty} C_{m,n} g(t - n\alpha) e^{i2\pi m\beta(t-n\alpha)},$$

where α and β are positive, with $\alpha\beta \leq 1$. This representation shows that the signal is to be expanded into *time-shifted* and *frequency-shifted* versions of the window. Therefore, *the application will dictate the choice of the window.* Indeed, this is the basic point [4] for analyzing transient signals. Since they consider a *transient signal* as a signal whose duration is short compared to the observation window, their basic idea is to replace the original Gaussian window of Gabor by the one-sided exponential function: $g(t) = \sqrt{2\lambda} e^{-\lambda t} u(t)$ to better follow transient signals with a sudden "on" time and subsequent exponential decay. Here $u(t)$ is the unit step function and "the parameter λ is used to control the effective width of the window" [4].

The use of the Gabor transform with this window is shown in the following DF simulation. A 10-sensor linear array is laid along the x-axis and each sensor is spaced one-half wave length at 11 Hertz with the first sensor located at the origin. An 11-Hertz plane-wave signal is impinging broadside to the array (azimuth $\theta = 90°$) with an amplitude of 1/10. The signal is corrupted by i.i.d. Gaussian noise $\mathcal{N}(0,1)$ at each sensor. In addition, five one-sided decaying transients were added to the environment (α=1, β=1, λ=1) and relevant parameters are displayed in Table 2: A total of

Table 2: Parameters for Gabor Transients

index	time delay (sec)	azimuth (deg)	frequency (Hertz)
1	13	62	12
2	23	63	12
3	21	110	10
4	5	64	12
5	10	80	13

1,024 array snapshots were collected during the time interval of $0 \leq t \leq 32$ seconds at a sampling rate of 32 Hertz. Figure 2 plots the 11-Hertz signal, the Gaussian noise, and the five transients at the first sensor. Figure 3 is a plot of the discrete Gabor transform of the output of first sensor. The time axis starts at time $t = 0$ in the leftmost corner and moves in one-second increments to the uppermost corner. The frequency axis starts at $f = 0$ in the leftmost corner and moves in one-Hertz increments to the lowest corner. The five transients are clearly displayed.

The effect of the transients on the MVDR DF is shown in Figure 4. MVDR used 11 Hertz in an attempt to find the weak 11-Hertz signal but the transients swamp the output. The transients were removed by taking the Gabor transform of each sensor's output, finding those coefficients exceeding three standard deviations of the Gabor transform, and then subtracting

the corresponding Gabor transients (weighted by its Gabor coefficient). Thus, the Gabor transform functioned as a pre-filter and the resulting array output was passed to the DF. With the transients removed, the MVDR DF located the 11-Hertz signal.

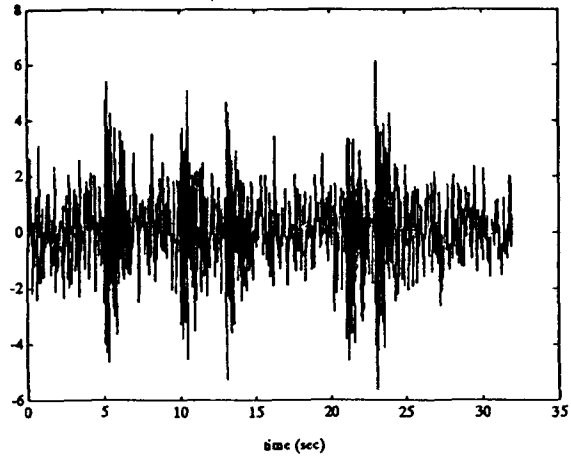

Figure 2: **Time Series of the First Sensor** — The 11-Hertz signal at 1/10 amplitude, additive $\mathcal{N}(0,1)$ noise, and the five Gabor transients.

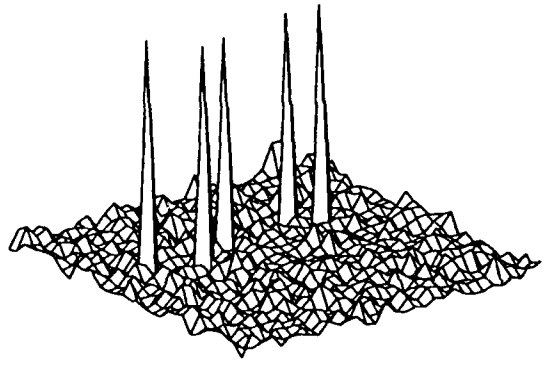

Figure 3: **Gabor Transform of the Time Series of the First Sensor** — The 11-Hertz signal at 1/10 amplitude, additive $\mathcal{N}(0,1)$ noise, and the five Gabor transients.

5 DF via the WVD

This section shows how one *preliminary* estimate of the Wigner-Ville Distribution (WVD) of the array output can be used to DF a source in both time and frequency. This approach is different from that of Swindlehurst and Kailath [21] in which a *spatial* WVD was used to handle the near-field effects and produced both bearing and range estimates. Instead, we show how to use the WVD to DF on a source in the far field, provided the signal admits a WVD sufficiently different from the background noise at a particular time

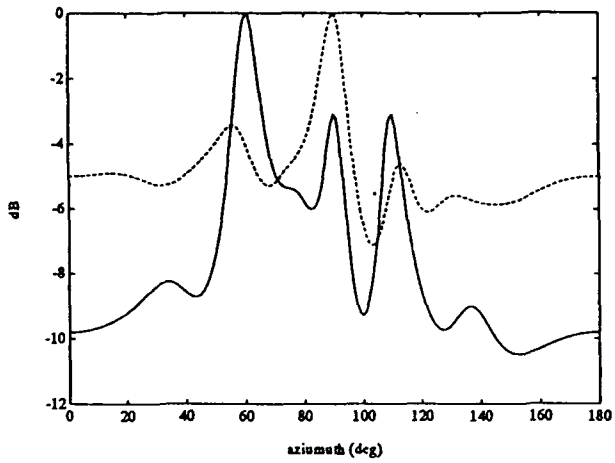

Figure 4: **MVDR using a Gabor Prefilter** — An 11-Hertz signal at 1/10 amplitude from 90° azimuth, additive $\mathcal{N}(0,1)$ noise, and the five Gabor transients. The CSD was estimated at 11 Hertz by averaging 32-sample blocks of the 1,024 array snapshots. The solid line is MVDR without the Gabor prefilter and the dashed is MVDR with the Gabor prefilter.

and frequency. As such, this approach could be used to DF on transients.

Given two analytic signals $x(t)$ and $y(t)$, their cross Wigner-Ville Distribution (XWVD) is [2]:

$$W(x,y;t,f) = \int_{-\infty}^{\infty} e^{-i2\pi f} x(t+\tau/2)\bar{y}(t-\tau/2)d\tau.$$

Consider the case of the array output when only one analytic signal is present from the direction $\mathbf{u}_0$. Then $\mathbf{x}(t) = [s(t+\tau_m(\mathbf{u}_0))]$. The XWVD of the mth and m'th sensor outputs is:

$$W(x_m, x_{m'}; t, f) = e^{i2\pi f(\tau_m(\mathbf{u}_0)-\tau_{m'}(\mathbf{u}_0))} \times \; W(s,s;t+\tau_m(\mathbf{u}_0)/2+\tau_{m'}(\mathbf{u}_0)/2, f).$$

If the XWVD is smoothed in time, then three observations can be made: First, if the time lags are relatively small with respect to the smoothing window, then the phase term is not affected while the time-shifted WVD of the signal may be approximated by the WVD of the signal. In matrix form, we get the estimate of the WVD of the array:

$$\widetilde{W}(\mathbf{x},\mathbf{x};t,f) \approx \mathbf{a}(f,\mathbf{u}_0)\mathbf{a}(f,\mathbf{u}_0)^H W(s,s;t,f),$$

where $\widetilde{W}$ denotes the smoothed WVD of the array output. Second, if noise is present and distributes in a uniform and zero-mean fashion over the time-frequency plane, then the smoothing should have the effect of providing a biased estimate of the WVD of the array but with a lower variance than the "raw" WVD. Third, the form of the estimate permits the application of subspace methods.

The following simulation supports these claims. The 10-sensor linear array spaced at 1/2 wavelength

(f = 11 Hertz) is receiving chirp signals from two sources: one source is broadside to the array (azimuth $\theta = 90°$). and transmits a four-second chirp. The chirp starts at time $t = 0$ at 16 Hertz and sweeps down at 4 Hz/sec. The second source is located at $\theta = 60°$ azimuth and transmits a chirp sweeping up at 4 Hz/sec starting from 0 Hertz. Sensor noise was modeled as i.i.d $\mathcal{N}(0,1)$. A total of N=128 array snapshots were collected at a 32 Hertz sample rate. Figure 5 plots conventional DF at 11 Hertz, the conventional WVD DF, and the MUSIC WVD (one signal). Both WVD DF used time $t = 1.25$ seconds and $f = 11$ Hertz. The conventional DF estimated the CSD matrix using 32-sample time blocks. The XWVD was estimated an FFT size of 64 and rectangular 8-point time-smoothing. The figure shows that both the WVD DF distinguish the two sources while the conventional DF also shows that there are two signals at 11 Hertz at 60° and 90° azimuth.

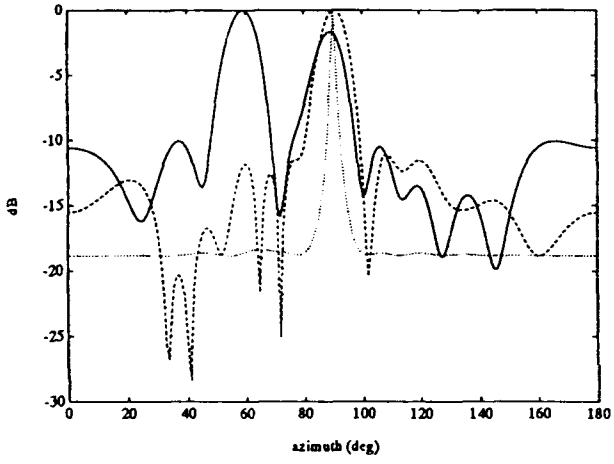

Figure 5: **WVD DF on Two Chirps** — One chirp at 90° azimuth sweeping down from 16 Hertz at -4 Hz/sec. The second chirp at 60° azimuth sweeping up from 0 Hertz at +4 Hz/sec. The solid line is the classical DF, the dashed line is classical WVD DF, and the dotted line is the MUSIC WVD DF (one signal).

6 DF on Cyclostationary Signals

The fundamental stumbling block in treating non-stationary time series is the lack of either a sample ensemble (which would permit a consistent estimation of the CSD matrix), or an ergodic theorem (which can produce a consistent estimate from a sufficiently long realization of the time series). While there is a large literature of attacks on non-stationary time series (see Priestley [17] for an accessible survey), this section will consider harmonizable, cyclostationary time series. These assumptions will permit the estimation of the CSD matrix and readily apply to DF.

Cyclostationary time series have been undergoing an extensive development in the last decade. (the April 1991 issue of the *IEEE Signal Processing Magazine* is devoted to cyclostationary processing). In particular, we single out the excellent Ph.D thesis of Schell [20] which exploits cyclostationarity to perform DF using subspace methods and has performed a Cramer-Rao lower bound analysis. Another approach to DF can be made using spectral estimators obtained by Hurd [7], [8] and is the subject of this section.

Definition 6.1 [15, page 226] A random process $\{x(t)\}$ is called cyclostationary of period $T > 0$ for which the mean and covariance functions are periodic: for all times t, t_1, and t_2, there holds $E[x(t+T)] = E[x(t)]$ and $R_x(t_1, t_2) = R_x(t_1 + T, t_2 + T)$.

Definition 6.2 [12] A random process $\{x(t)\}$ is called (strongly) harmonizable provided it can be represented in quadratic mean for every time t by the integral

$$x(t) = \int_{-\infty}^{\infty} e^{i2\pi f t} dX(f)$$

where X is a random measure for which the spectral measure defined by $P_x(A \times B) = E[X(A)\overline{X(B)}]$ is of bounded variation.

Hurd [7] points out that when $\{x(t)\}$ is both cyclostationary and harmonizable then the spectrum $P_x(f_1, f_2)$ is confined to diagonal lines in the $f_1 \times f_2$ plane which are parallel to the main diagonal and spaced $1/T$ Hertz apart. In particular, stationary noise will be confined to the main diagonal (f_1=f_2) and DF using $f_1 \neq f_2$ should permit noise suppression. The DF assumptions are as follows:

Assumption 6.1 Single Cyclostationary source, uncorrelated noise:

1. the plane wave signal $s(t)$ is a strongly harmonizable, cyclostationary random process.

2. the noise $\mathbf{z}(t)$ is zero-mean, WSS.

3. the signal $s(t)$ and the sensor noise are uncorrelated.

Since the noise vector $\mathbf{z}(t)$ is WSS and signal $s(t)$ is strongly harmonizable, then the array Then the array output $\mathbf{x}(t)$ is harmonizable with a Fourier measure given by $d\mathbf{X}(f) = \mathbf{a}(f, \mathbf{u}_0)dS(f) + d\mathbf{Z}(f)$, where only $\mathbf{Z}(f)$ is orthogonally scattered. From this representation, the CSD matrix of the array has the form:

$$\begin{aligned} dP_{\mathbf{X}}(f_1, f_2) &= E[d\mathbf{X}(f_1)d\mathbf{X}(f_2)^H] \\ &= dP_s(f_1, f_2)\mathbf{a}(f_1, \mathbf{u}_0)\mathbf{a}(f_2, \mathbf{u}_0)^H + dP_{\mathbf{n}}(f_1, f_2). \end{aligned}$$

Note the following: the noise CSD matrix is supported only on the line of zero frequency difference; the extension to subspace algorithms appears straight-forward; the CSD matrix can be estimated by averaging outer products of FFT vectors of the time segments of the data if the period T is known.

The following simulation examines these claims. A 10-sensor linear array spaced at 1/2 wavelength (f = 11 Hertz) is receiving two signals: the first is a cyclostationary signal generated by amplitude-modulating $\mathcal{N}(0,1)$ noise at 4 Hertz. This AM signal is normalized by setting the sample standard deviation to one and arrives broadside to the array (90°

azimuth). The second signal is an 11-Hertz complex exponential arriving at 75° azimuth. Sensor noise is i.i.d. $\mathcal{N}(0,1)$. A total of 256 array snapshots were collected at a 128 Hertz sample rate. The classical DF estimated the CSD matrix by averaging 32-point blocks at 11 Hertz. The cyclostationary DF worked by picking a look direction and then feeding the output of the conventional delay-sum beamformer into a estimator of the two-dimensional spectrum $P_x(f_1, f_2)$ at the point $(f_1, f_2) = (11, 15)$ Hertz. The spectral estimator performed diagonal smoothing by averaging 11 diagonal bins spaced 0.5 Hertz apart centered about at (11,15). The results are displayed in figure 6. The classical DF localizes the 11-Hertz signal while the cyclostationary DF locates the AM signal.

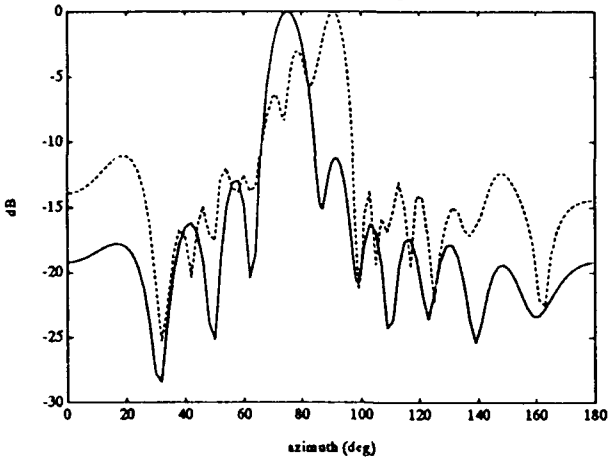

Figure 6: **DF on Cyclostationary Signals** — Gaussian AM signal at 90° azimuth; 11 Hertz signal at 75° azimuth. The solid line is the classical DF; the dashed line is the cyclostationary DF.

7 DF on a Chaotic Signal

In the past decade, there has been a surge of publications in chaotic systems. Of particular interest for sonar applications, we single out the work of K. Karagiannis [11] which observed chaotic behavior in the noise generated by rattling gearboxes. One basic model of chaotic behavior is the conventional logistic map (CLM) [23]:

$$x(t+1) = \mu x(t)(1 - x(t)).$$

One stochastic generalization of the CLM is the Model 2 of [6]: for $t = 1, 2, \ldots$

$$x(t+1) = k(a,b)x(t)^a(1 - x(t))^b u(t+1)^c,$$

where a, b, and c are non-negative, $\{u(t)\}$ are independent and identically distributed uniformly on the interval $[0,1]$, $k(a,b) = (a+b)^{a+b}/(a^a b^b)$, and the initial value is set as $x(0) = u(0)^c$. Estimators of a, b, c were obtained and it was observed that Model 2 provided a good fit to time series generated by the CLM.

This section demonstrates that the Model 2 estimators of a, b, and c can apply to source localization. The basic idea is to assume that a signal $s(t)$ is of the form of the Model 2. A look direction is picked and the time series resulting from the conventional delay-sum beamforming is fed into the estimation scheme. The one-step mean-squared prediction error is calculated and its reciprocal is plotted as a function of the look direction. If the look direction matches the signal direction, then a good fit of the signal is obtained which results in a small prediction error. Otherwise, a poor fit occurs which results in a large prediction error. We compare this Fractal DF with the conventional DF and the MUSIC DF in the following simulations.

We use a 10-sensor linear array with 1/2 wavelength spacing (f = 11 Hertz). One signal is placed broadside to the array (azimuth $\theta = 90°$) and is generated from the CLM ($\mu = 4$, $s(0) = 1/3$). An second signal was generated from the CLM and arrives on the array from 95° azimuth. The arrival was simulated using the Fourier method: the FFT of the time series was multiplied by the appropriate phase for each sensor and the inverse FFT determined the signal at each sensor. Sensor noise was modeled as i.i.d zero mean Gaussian with the standard deviation set so the SNR=1. A total of N=128 array snapshots were collected at a 100 Hertz sample rate. The Classical and MUSIC DF were operated at 11 Hertz and the CSD matrix was estimated using 32-point block-averaging. MUSIC assumed two sources. All DFs locate the source at 90° azimuth though the beamwidth of the fractal DF is much narrower than the other DFs. The results are shown in figure 7. The Conventional and MUSIC DFs could not resolve this sources, but the Fractal DF is correctly indicating the signal directions at 90° and 95° azimuth.

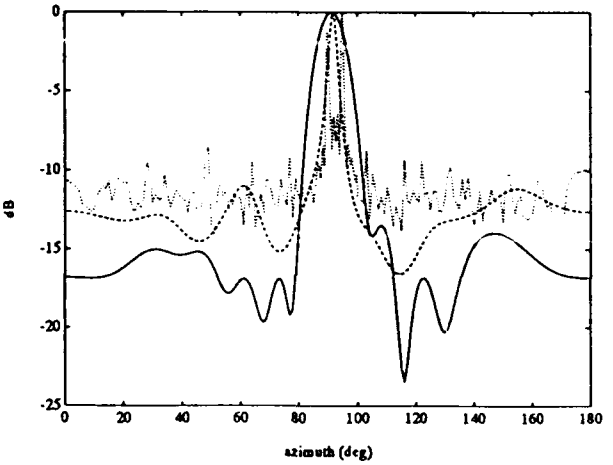

Figure 7: **DF on a Two Chaotic Signals** — Two CLM signals at 90° and 95° azimuth. The solid line is the classical DF, the dashed line is MUSIC, and the dotted line is the Fractal DF.

8 Conclusions

The preceding sections have shown that Johnson's [10] approach to bearing estimation as form of spectral estimation readily generalizes whenever a statistically consistent estimator of a signal attribute can be found.

References

[1] Allen, J. C., *Direction-Finding and Database Techniques*, NOSC Technical Note 1657, Naval Ocean Systems Center, San Diego, CA 92152, 1990

[2] Flandrin, P., "A Time-Frequency Formulation of Optimum Detection", *IEEE Transactions on ASSP*, Volume 36, Number 1, pages 1377–1384, 1988

[3] Forster, P. and C. L. Nikias, "Bearing Estimation in the Bispectrum Domain", *IEEE Transactions on Signal Processing*, Volume 39, Number 9, pages 1994–2006, 1991

[4] Friedlander, B. and B. Porat, "Detection of Transient Signal by the Gabor Representation", *IEEE Transactions on ASSP*, Volume 37, Number 2, pages 169–179, 1989

[5] Gabr, M. M. "On the Third-Order Moment Structure and Bispectral Analysis of Some Bilinear Time Series", *Journal of Time Series Analysis*, Volume 9, Number 1, pages 11–20, 1988

[6] Gerr, N. L. and J. C. Allen, "Multiplicative Models for Bounded Time Series", Submitted to the *Journal of Time Series Analysis*, September, 1991

[7] Hurd, H. L., "Representation of Strongly Harmonizable Periodically Correlated Processes and Their Covariances", *Journal of Multivariate Analysis*, Volume 29, Number 1, pages 53–67, 1989

[8] Hurd, H. L., "Nonparametric Time Series Analysis for Periodically Correlated Processes", *IEEE Transactions on Information Theory*, Volume 35, Number 2, pages 350–359, 1989

[9] Hurd, H. L. and N. L. Gerr, "Graphical Methods for Determining the Presence of Periodic Correlation", *preprint*, 1990

[10] Johnson, D. L., "The Application of Spectral Estimation Methods to Bearing Estimation", *Proceedings of the IEEE*, Volume 70, Number 90, pages 1018–1028, 1982

[11] Karagiannis, K., "Rattling Vibrations in Gearboxes", *Lecture Notes in Physics, Volume 355*, Springer-Verlag, Berlin-New York, pages 175–195, 1990

[12] Loève, M., *Probability Theory*, D. Van Nostrand Company, Inc., New York, 1963

[13] Mendel, J. M., "Tutorial on Higher-Order Statistics (Spectra) in Signal Processing and System Theory: Theoretical Results and Some Applications", *Proceedings of the IEEE*, Volume 79, Number 3, pages 278–304, 1991

[14] Nikias, C. L. and M. R. Raghuveer, "Bispectrum Estimation: A Digital Signal Processing Framework", *Proceedings of the IEEE*, Volume 75, Number 7, pages 869–891, 1987

[15] Papoulis, A., *Probability, Random Variables, and Stochastic Processes*, second edition, McGraw-Hill, New York, 1984

[16] Porat B. and B. Friedlander, "Direction Finding Algorithms Based on High-Order Statistics", *IEEE Transactions on Signal Processing*, Volume 39, Number 9, pages 2016–2024, 1991

[17] Priestley, M. B., *Non-Linear and Non-Stationary Time Series Analysis*, Academic Press, New York, 1988

[18] Rao, T. Subba and M. M. Gabr, *An Introduction to Bispectral Analysis and Bilinear Time Series Models*, Lecture Notes in Statistics, Volume 24, Springer-Verlag, New York, 1984

[19] Rosenblatt, M., *Stationary Sequences and Random Fields*, Birkhäuser, Boston, 1985

[20] Schell, S. V., *Exploitation of Spectral Correlation for Signal-Selective Direction Finding*, Ph.D thesis, Department of Electrical Engineering and Computer Science, University of California, Davis, 1990

[21] Swindlehurst, A. L. and T. Kailath, "Passive Direction-of-Arrival and Range Estimation for Near-Field Sources", *Fourth Annual ASSP Workshop of Spectrum Estimation and Modeling*, Spring Hill Conference Center, Minneapolis, Minnesota, IEEE Inc., pages 123–128, August 3–5, 1988

[22] Squire, B., *A Tutorial Survey of Time-Frequency Analysis and Applications*, Linear Measurements, 1991

[23] Thompson, J. M. T. and H. B. Stewart, *Nonlinear Dynamics and Chaos*, John-Wiley and Sons, New York, 1986